International Journal of Research and Development in Applied Science and Engineering (IJRDASE)

Human Brain MRI Quality Improvement by Weighted Sum and Multi Echo Frequency Contrast Enhancement

Sunit Kumar Trivedi
Electronics & Communication Engineering,
Integral University, Lucknow, India
sktrivedi80@yahoo.co.in

Shailendra Kumar Singh
Electronics & Communication Engineering,
Integral University, Lucknow, India
shail288@gmail.com

***Abstract*--A very effective technique is developed for contrast enhancement in multi echo magnetic resonance imaging (MRI) data of horizontal and vertical section of human brain by utilizing the field maps derived from multi-echo gradient-echo images. The MRI images consist of noise due to different off-resonance factors cased by field inhomogeneity, eddy current effect, radio frequency pulse frequency offset, and chemical shift effect. These effects can be significantly reduced to a great extent by suitable image enhancement algorithm. We have applied WSA and MEFIC algorithm for brain MRI image enhancement without disturbing the phase discontinuities in the derived field map. Results demonstrate that the enhancement performance of this method helps very magnificently in reducing the geometrical distortions in echo images.**

***Key words--Echo planar imaging (EPI), Image enhancement, N-D FFT, MRI, Multi echo image*.**

1. Introduction:

Functional magnetic resonance imaging (FMRI) measures changes in blood oxygenation and blood volume that result from neural activity [1]. Deoxygenated haemoglobin acts as an paramagnetic agent, so a reduction in the concentration of it increases the weighted magnetic resonance signal. A typical fMRI experiment measures the correlation between the fMRI response and a stimulus. From this, scientists finds informations to infer something about neural activity. Often it is assumed that there is a simple and direct relationship between neural activity and fMRI response, but the nature of this relationship remains unclear. The goal of the research reported in this thesis is to enhance the quality of MRI image of brain to clearly estimate the neural activity. The vascular source of the MRI signal places important limits on the technique. Because the hemodynamic response is sluggish, perhaps the MRI response is proportional to the local average neural activity, averaged over a small region of the brain and averaged over a period of time. We will refer to this as the "linear fourier transform model" of MRI of brain images. The linear transform model, specialized for a visual area of the brain, is depicted in Figure 1. According to this model, neural activity is a nonlinear function of the contrast of a visual stimulus, but fMRI response is a linear transform (averaged over time) of the neural activity in V1. Noise might be introduced at each stage of the process, but the effects of these individual noises can be summarized by a single noise source that is added to the output. To date, this linear transform model of fMRI response has not been tested, despite the fact that some studies rely explicitly on the linear model for their data analysis [2]. The sequence of events from neural response to fMRI response is complicated and only partially understood. It is unlikely that the complex interactions among neurons, hemodynamics, and the MR scanner would result in a precisely linear transform. However, the linear transform model might be a reasonable approximation of these complex interactions. The linear transform model is attractive because, if it were correct, it would greatly simplify the analysis and interpretation of fMRI data. Most important, it would provide confidence in inferences made about neural activity. In addition, the relationship between neural activity and fMRI response would be characterized completely and simply by the fMRI "impulse–response function," that is, the fMRI response resulting from a brief, spatially localized pulse of neural activity. The fMRI impulse–response function would allow one to predict the fMRI response evoked by any pattern of neural activity. This would help in experimental design, for example, in choosing the temporal duration of a visual stimulus when measuring fMRI responses in visual cortex. According to the linear transform model, the fMRI impulse–response function would characterize completely both the spatial and the temporal averaging of the neural activity. This work also concentrates only on primary visual cortex (V1), although the approach certainly may be used for studying other areas as well. Note, however, that the spatial and temporal averaging may be different in different brain areas, especially since the vasculature seems to be specialized in particular brain areas (e.g., in V1) [3]. Although these tests can not prove the correctness of the linear transform model, they might have been used to reject the model. Because the linear transform model is consistent with our data, we proceeded to estimate the temporal fMRI impulse–response function and the underlying (presumably neural) contrast–response function of human V1.

2. Literature Review:

Christian Denk et. al. (2010) [7], extend susceptibility weighted imaging (SWI) to multiple echoes with an adapted homodyne filtering of phase images for the computation of venograms with improved signal to noise ratio (SNR) and contrast to noise ratio (CNR) and to produce high resolution maps of R2* relaxation. Three-dimensional multi echo gradient echo data were acquired with five equidistant echoes ranging from 13 to 41 ms. The phase images of each echo were filtered with filter parameters adjusted to the echo time, converted into a phase mask, and combined with the corresponding magnitude images to obtain susceptibility weighted images. The individual images were then averaged.

conventional single echo data were acquired for comparison. Maps of R2* relaxation rates were computed from the magnitude data. Field maps derived from the phase data were used to correct R2* for the influences from background inhomogeneities of the static magnetic field. Compared with the single echo images, the combined images had an increase in SNR by 46% and an improvement in CNR by 34 to 80%, improved visibility of small venous vessels and reduced blurring along the readout direction. The R2* values of different tissue types are in good agreement with values from the literature. Acquisition of SWI with multiple echoes leads to an increase in SNR and CNR and it allows the computation of high resolution maps of R2* relaxation.

Karin Shmueli et. al. (2009) [6], according to them phase images in susceptibility-weighted MRI provide excellent contrast. However, the phase is affected by tissue geometry and orientation relative to the main magnetic field (B0) and phase changes extend beyond areas of altered susceptibility. Magnetic susceptibility, on the other hand, is an intrinsic tissue property, closely reflecting tissue composition. Therefore, recently developed inverse Fourier-based methods were applied to calculate susceptibility maps from high-resolution phase images acquired at a single orientation at 7 Tesla in the human brain (in vivo and fixed) and at 11.7 Tesla in fixed marmoset brain. In susceptibility images, the contrast of cortical layers was more consistent than in phase images and was independent of the structures' orientation relative to B0. The contrast of iron-rich deep-brain structures (red nucleus and substantia nigra) in susceptibility images agreed more closely with iron-dominated R2* images than the phase image contrast which extended outside the structures. The mean susceptibility in these regions was significantly correlated with their estimated iron content. Susceptibility maps calculated using this method overcome the orientation-dependence and non-locality of phase image contrast and seem to reflect underlying tissue composition. Susceptibility images should be easier to interpret than phase images and could improve our understanding of the sources of susceptibility contrast.

Recent in vivo MRI studies at 7.0 T have demonstrated by **Tie-Qiang Li et. al. (2009) [5],** to extensive heterogeneity of T2* relaxation in white matter of the human brain. In order to study the origin of this heterogeneity, we performed T2* measurements at 1.5, 3.0, and 7.0 T in normal volunteers. Formalin-fixed brain tissue specimens were also studied using T2*-weighted MRI, histological staining, chemical analysis, and electron microscopy. We found that T2* relaxation rate (R2*=1/ T2*) in white matter in living human brain is linearly dependent on the main magnetic field strength and the T2* heterogeneity in white matter observed at 7.0 T can also be detected, albeit weaker, at 1.5 and 3.0 T. The T2* heterogeneity exists also in white matter of the formalin fixed brain tissue specimens, with prominent differences between the major fiber bundles such as the cingulum and the superior corona radiada. The white matter specimen with substantial difference in T2*have no significant difference in the total iron content as determined by chemical analysis. On the other hand, evidence from histological staining and electron microscopy demonstrate these tissue specimen have apparent difference in myelin content and microstructure.

In vivo MRI-derived measurements of human cerebral cortex thickness are providing novel insights into normal and abnormal neuroanatomy, but little is known about their reliability. **Xiao Han et. al. (2006) [4],** investigated how the reliability of cortical thickness measurements is affected by MRI instrument-related factors, including scanner field strength, manufacturer, upgrade and pulse sequence. Several data processing factors were also studied. Two test –retest data sets were analyzed: 1) 15 healthy older subjects scanned four times at 2-week intervals on three scanners; 2) 5 subjects scanned before and after a major scanner upgrade. Within-scanner variability of global cortical thickness measurements was <0.03 mm, and the point-wise standard deviation of measurement error was approximately 0.12 mm. Variability was 0.15 mm and 0.17 mm in average, respectively, for cross-scanner (Siemens/GE) and cross-field strength (1.5 T/3 T) comparisons. Scanner upgrade did not increase variability nor introduce bias. Measurements across field strength, however, were slightly biased (thicker at 3 T). The number of (single vs. multiple averaged) acquisitions had a negligible effect on reliability, but the use of a different pulse sequence had a larger impact, as did different parameters employed in data processing. Sample size estimates indicate that regional cortical thickness difference of 0.2 mm between two different groups could be identified with as few as 7 subjects per group, and a difference of 0.1 mm could be detected with 26 subjects per group. These results demonstrate that MRI-derived cortical thickness measures are highly reliable when MRI instrument and data processing factors are controlled but that it is important to consider these factors in the design of multi-site or longitudinal studies, such as clinical drug trials.

3. Proposed Methodology:

We have taken set of 4 images of MRI data for applying the algorithm of generation of enhanced image from set of four MRI images. For generation of enhanced images two different algorithms are developed, first algorithm is named as weighted summing average (WSA) and another is named as Multi Echo Fourier Image Contrast (MEFIC) technique.Both the algorithms are explained one by one in upcoming section.

A. Weighted summing average (WSA):

In this algorithm first of all we take set of some images from the stack of MRI data having features of multi echo imaging. Let this set of images is I=[I1,I2,I3...Ik] having k images in each set. There after we select any image from the set I which is to be enhanced say Ii. Now we assigns the weight to each image of the set I such that the Ii^{th} image has highest weightage. Let the weight matrix taken as W=[w1 w2 w3...wi....wk].Such that wi> w1 to wk weights.If the size of each image is MxN then all the the images are reshaped and combined to form a single image of MxN rows and k columns. For this prupose each image matrix of MxN size is reshaped to 1 D array of M*N rows and 1 column.

$$Ia = \begin{bmatrix} a1 & a2 & a3 \\ a4 & a5 & a6 \\ a7 & a8 & a9 \end{bmatrix},$$

$$Ib = \begin{bmatrix} b1 & b2 & b3 \\ b4 & b5 & b6 \\ b7 & b8 & b9 \end{bmatrix},$$

$$Ic = \begin{bmatrix} c1 & c2 & c3 \\ c4 & c5 & c6 \\ c7 & c8 & c9 \end{bmatrix},$$

$$Id = \begin{bmatrix} d1 & d2 & d3 \\ d4 & d5 & d6 \\ d7 & d8 & d9 \end{bmatrix}$$

$$W=[w1 \quad w2 \quad w3 \quad w4]$$

$$I=\begin{bmatrix} a1 & b1 & c1 & d1 \\ a2 & b2 & c2 & d2 \\ a3 & b3 & c3 & d3 \\ a4 & b4 & c4 & d4 \\ a5 & b5 & c5 & d5 \\ a6 & b6 & c6 & d6 \\ a7 & b7 & c7 & d7 \\ a8 & b8 & c8 & d8 \\ a9 & b9 & c9 & d9 \end{bmatrix}$$

AS shown above that Ia, Ib , Ic and Id are the set of 4 images i.e k=4 and let the weight matrix is w and the reshaped image is I made from Ia, Ib, Ic and Id.After generating the I image we multiplies the transpose of w to the I to get and weighted image $Iw=I*w^t$.The Iw image is normalized by dividing it to sum of weights as given below:

$$\mathbf{Iw=Iw/\sum W}$$

After normalization the Iw is reshaped to its original dimension of MxN this represents the enhanced MRI image after applying this weighted summing average (WSA) algorithm.

B. Multi Echo Fourier Image Contrast (MEFIC):

In this algorithm first of all we take set of some images from the stack of MRI data having features of multi echo imaging. Let this set of images is I=[I1,I2,I3...Ik] having k images in each set. There after this algorithm selects last image from the set 'I' this is to be enhanced. If we have taken k images then the k^{th} - dimension FFT will be applied on the image stack.

The transformed image will also consist of k^{th} dimension matrices having exact size as the set 'I' but it will have complex Fourier coefficients of the basic images that are to be enhanced. In this matrix set of transformed data we take the magnitude of the complex set .Out of this magnitude data set we pick only those coefficients which have maximum value at each pixel address among the all 1 to k magnitude data matrix in this way the resultant is a 2-D matrix having only magnitude of most significant coefficients. This matrix is the enhanced image obtained by MEFIC method.

4. Result and Discussion:

We have considered two different kinds of MRI images of brain for examining the performance of our algorithm in respect of the image enhancement. These images are taken in this results analysis are horizontal cross section of brain MRI scan named as wmri.mat and vertical cross section named as series8.

A. Image Enhancement of horizontal cross-section of brain MRI:

In this section we will discuss the results obtained for wmri.mat image data set for figure 1.1 MRI scans. We have applied both WSA and MEFIC algorithm for this data set and the generated results are discussed below:

i. Enhancement using WSA: The description about the WSA algorithm is given in chapter 3 of methodology. The weights for enhancing image are changed for various values and we have got best result at the weight having value weights=[0.2 0.2 0.4 0.2]for the wmri.mat data. In this case weight of third image is 0.4 and total sum of weights is 1 at this value the brightness of enhanced image will be closer to original set where as the third image will have higher information content along with the informations of 1^{st} , 2^{nd} and 4^{th} image. The results of the WSA algorithm are shown in fig. 1. Fig 1(a) shows the original images in there stack order. We have taken three different values of weights these are [0.2 0.2 0.4 0.2 the images at this weights is shown in fig. 1(b).

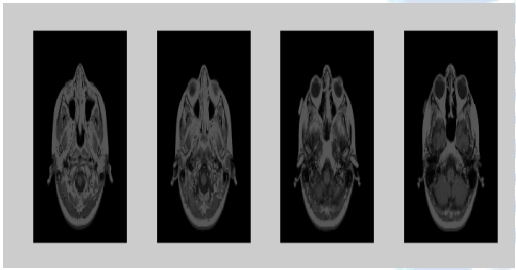

Fig. 1(a). Initial four Brain MRI image obtained from wmri.mat data image stack.

enhanced image

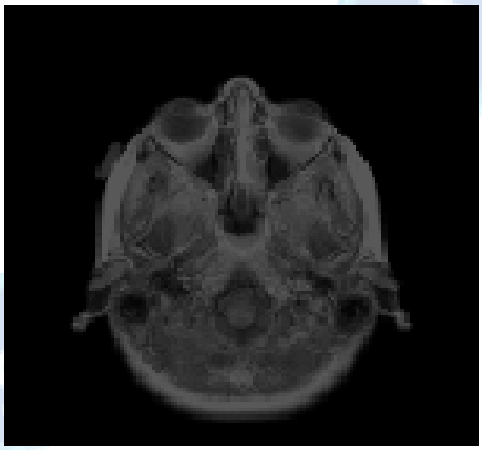

Fig. 1(b). Enhanced image by Weighted sum avg method at weight [0.2 0.2 0.4 0.2]

ii. Enhancement using MEFIC:

The description about the MFIC algorithm is given in chapter 3 of methodology. There is no need of weights for enhancing image. We have got best enhancement result for the wmri.mat data as given in fig. 2. In this case the last image is the enhanced image and hence out of the original the fourth

image will have higher information content along with the information of 1st , 2nd and 3rd image in enhanced image. The results of the MEFIC algorithm are shown in fig 2 for this wmri.mat data. Fig 2(a) shows the absolute value or magnitudes of FFT images as per the original stack order. Fig. 2(b) shows the fourth enhanced image after combining the images of fig. 2(a) and on taking inverse FFT.

Fig. 2(b) is the resultant enhanced image after applying the MEFIC algorithm. We can see that the enhanced image by MEFIC his very rich in contrast and a large amount of information can be seen in this image which composed of collective information of all the four images.

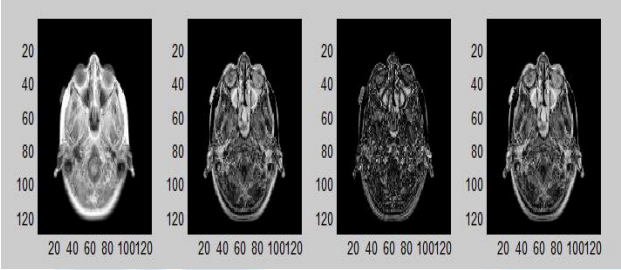

Fig 2(a):Magnitude images of FFT of images shown in fig 1(a).

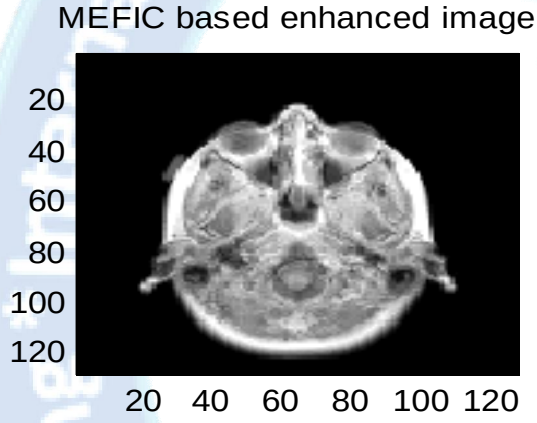

Fig 2(b): Enhanced image obtained by MEFIC method.

B. Image Enhancement of vertical cross-section of brain MRI:

In this section we will discuss the results obtained for series8 image data set for fig 1 MRI scans. We have applied both WSA and MEFIC algorithm for this data set and the generated results are discussed below:

i. Enhancement using WSA:

The description about the WSA algorithm is given in part 3 of methodology. The weights for enhancing image are changed for various values and we have got best result at the weight having value weights [0.5 0.5 1.5 0.5] for the series8 data. In this case weight of third image is 1.5 and total sum of weights above than 1 at this value the brightness of enhanced image will be closer to original set where as the third image will have higher information content along with the informations of 1st , 2nd and 4th image. The results of the WSA algorithm are shown in fig. 3. Fig. 3 (a to d) shows the original images in there stack order. We have taken the various different values of weights and best result is found at the weight [0.5 0.5 1.5 0.5] as shown in fig. 3(e).

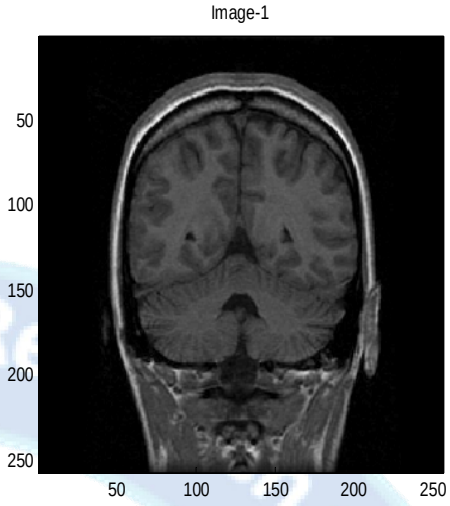

Fig. 3(a). Image 1 of coronal slices.

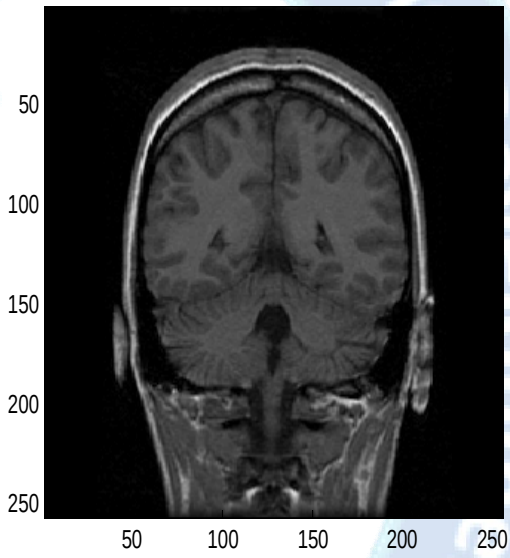

Fig. 3(b). Image 2 of coronal slices.

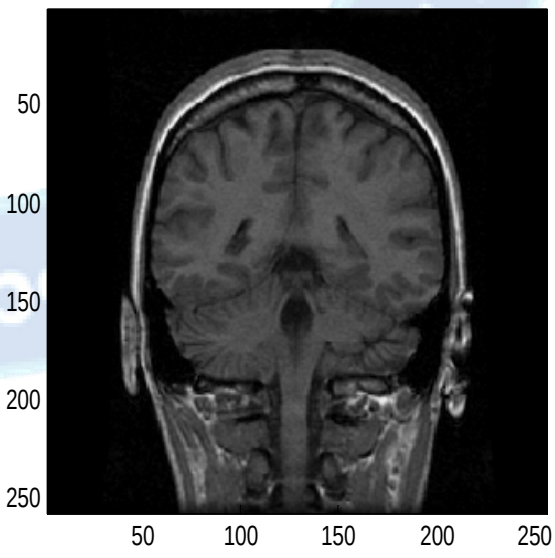

Fig. 3(c). Image 3 of coronal slices.

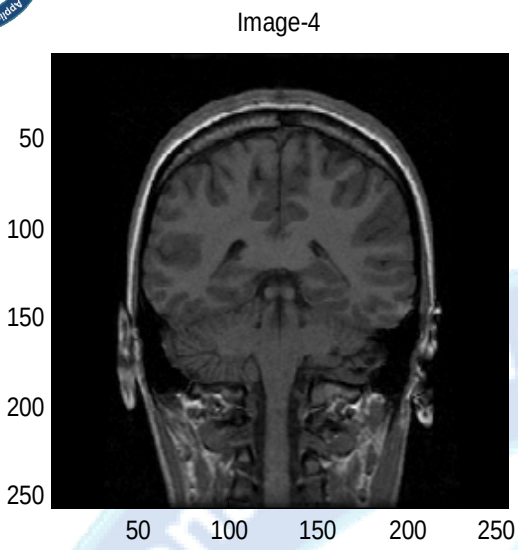

Fig. 3(d). Image 4 of coronal slices.

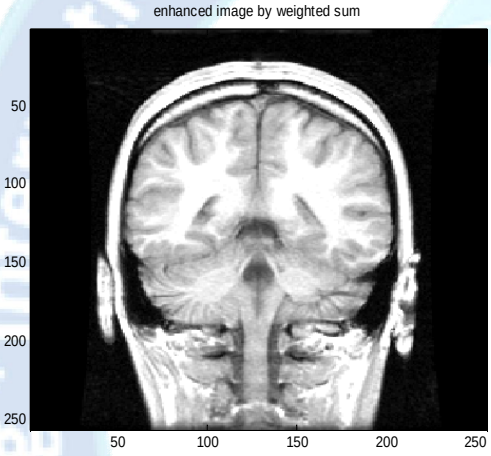

Fig. 3(e) : Enhanced image by Weighted sum averaging method at weight [0.5 0.5 1.5 0.5]

ii. Enhancement using MEFIC:

The description about the MFIC algorithm is given in chapter 3 of methodology. There is no need of weights for enhancing image. We have got best enhancement result for the series8 data as given in fig 3(f). In this case the last image is the enhanced image and hence out of the original the fourth image will have higher information content along with the information of 1st , 2nd and 3rd image in enhanced image. The results of the MEFIC algorithm are shown in fig. 3(f) for this series8 data.

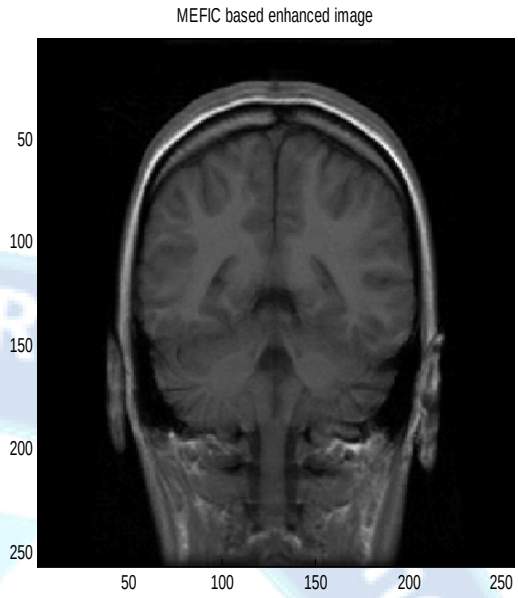

Fig 3(f). Enhanced image obtained by MEFIC method.

5. Conclusion

The use of active staining has revolutionized the field of magnetic resonance imaging by providing the acquisition of best quality resolution image data in a very short scan times. In the most of the MRI data the contrast in the actively-stained regions of human brain was very low due to the effect of T1-weighted contrast. These low contrast image acquisitions have posed problems in medical diagnosis due to signal decaying for the long TEs and the long scanning times is involved. The decay occurs slowly due to spin dephasing induced by diffusion through susceptibility gradients. With the implementation of WSA and MEFIC image enhancement algorithm on horizontal and vertical cross section brain MRI sequence we are able to obtain enhanced brain MRI image from the set of 4 low contrast image data.

References:

[1] Ogawa S, Tso-Ming L (1990) Magnetic resonance imaging of blood vessels at high fields: in vivo and in vitro measurements and image simulation. Magn Reson Med 16:9 –18.

[2] Friston KJ, Jezzard P, Turner R (1994) Analysis of function MRI time series. Hum Brain Mapp 1:153–171.

[3] Zheng D, LaMantia AS, Purves D (1991) Specialized vascularization of the primate visual cortex. J Neurosci 1991:2622–2629.

[4] Xiao Han et. al., "Reliability of MRI-derived measurements of human cerebral cortical thickness: The effects of field strength, scanner upgrade and manufacturer" doi:10.1016/j.neuroimage.2006.02.051.

[5] Tie-Qiang Li et. al., " Characterization of T2* Heterogeneity in Human Brain White Matter" Magn Reson Med. 2009 December ; 62(6): 1652–1657. doi:10.1002/mrm.22156.

[6] Karin Shmueli et. al., "Magnetic Susceptibility Mapping of Brain Tissue In Vivo Using MRI Phase Data" Magn Reson Med. 2009 December ; 62(6): 1510–1522. doi:10.1002/mrm.22135.

[7] Christian Denk et. al., " Susceptibility Weighted Imaging With Multiple Echoes", Journal Of Magnetic Resonance Imaging 31:185–191 (2010).